Application of the lifting line vortex wake method to dynamic load case simulations

K. Boorsma, M. Hartvelt and L.M. Orsi

ECN Wind Energy, Westerduinweg 3, 1755 LE Petten, The Netherlands

E-mail: boorsma@ecn.nl

Abstract. Within the EU AVATAR project, the added benefit of using the vortex line method is researched by calculating aero-elastic response for a variety of IEC load cases. A comparison is made to BEM to identify differences. Results are presented for yawed flow, extreme transient shear, half wake and turbulent inflow conditions. In addition to that also a dynamic pitch step case is performed including a comparison to experimental data. The aerodynamic code used for this purpose allows to easily switch between BEM and vortex line models whilst keeping the external input the same.

The comparison indicates that taking into account vortex wake models can yield a significantly different aero-elastic response compared to BEM models, often acting as a damper to fluctuations. As such estimated fatigue loads are reduced for selected load cases. Since the free vortex wake simulations come at a substantial increase of CPU-time, a hybrid approach prescribing the far wake is shown to offer a promising compromise.

1. Introduction

Uncertainty in aerodynamic load prediction is an important parameter driving the price of wind energy [1, 2]. Blade Element Momentum (BEM) theory is still the current standard for estimating the wind forces in load case calculations. The variety between the several engineering extensions used in different BEM implementations is huge [1, 2]. In addition to that, the assumption of radial independence of the annuli and the lack of wake modelling are well known shortcomings of this method. A physically more correct approach to model the rotor aerodynamics is presented by a vortex line method with a (free) vortex wake.

Application of vortex wake methods for evaluation of rotor aerodynamic loads has been researched for over a decade [3, 4, 5]. Previous work on this topic has focused on validation [6, 7], mainly by comparison to steady and rigid turbine wind tunnel measurements [8, 9] in axial and yawed flow. Where a good agreement between BEM, vortex wake and experiment was demonstrated in axial flow, vortex wake models show improved prediction of load variation in yawed flow. A comparison between several codes in sheared inflow [10] exposed the shortcomings in BEM methodology and superiority of vortex wake models dealing with non-uniformity in the rotor plane. Similar observations were made for individual pitch and pitch misalignment load cases [11, 12]. Performance in case of extreme coherent gust with direction change [11] was evaluated showing BEM to over predict maximum out of plane blade deflection up to 4% in comparison to the vortex wake code used.

Most of the previous applications of vortex wake models have focused at evaluating steady (time averaged) performance rather than dynamic load case performance and have not always

considered the flexibility of the turbine and its influence on the aerodynamics. The few attempts made in this direction are often hampered by limited spatial and temporal resolution, not allowing to calculate realistic statistics in terms of fatigue loading. Prescribing the wake convection instead of iterating out the full influence matrix (of all vortices) for each vortex point would significantly reduce the computational effort and good results were previously demonstrated [13]. More recently, introducing the effect of trailed vorticity variation in BEM [14] appeared to be a promising compromise between BEM and vortex theory.

Within the EU AVATAR project, the added benefit of using the vortex line method is researched by calculating aero-elastic response for a variety of dynamic IEC load cases. Here prescribing part of the wake together with the usage of parallel computing is employed to achieve this goal. Results will be presented for yawed flow, extreme transient shear, half wake and turbulent inflow conditions. In addition to that also a dynamic pitch step case is performed including a comparison to data from the New Mexico experiment. Firstly the methodology section describes the used code and its settings, after which the results are discussed followed by conclusions.

2. Methodology

The ECN Aero-Module [6] is used as aerodynamic solver for the current investigation. The two aerodynamic models included are the Blade Element Momentum (BEM) method similar to the implementation in PHATAS [15] and a free vortex wake code in the form of AWSM [3]. Both models are lifting line codes, i.e. they make use of aerodynamic look-up tables to evaluate airfoil performance. Several dynamic stall models, 3D correction models, wind modeling options and a module for calculating tower effects are included. The set-up allows to easily switch between the two aerodynamic models whilst keeping the external input the same, which is a prerequisite for a good comparison between them. The package is coupled to the FOCUS-Phatas simulation software [16] that solves the structural dynamics of a wind turbine, thus enabling full aero-elastic interaction.

2.1. Wake modeling

The ECN dynamic inflow model [17] has been implemented for usage with the BEM solver. This model adds another term to the axial momentum equation to account for the aerodynamic rotor 'inertia' in the case of pitch action, rotational speed variation or wind speed variation. The term is proportional to the time derivative of the annulus averaged axial rotor induction and has a dependency on the radial position.

AWSM models the wake geometry by convecting shed and trailing vorticity as depicted in Figure 1. Here the trailing vorticity accounts for the effects of spanwise circulation variation, whilst the shed vorticity accounts for the effects of bound vortex variation with time. As a result, effects due to dynamic inflow (e.g. pitch step), shed vorticity (e.g. aero-elastic instabilities), skewed wake, non-uniformities in the rotor plane (e.g. shear, individual pitch, non-coherent gusts) and variation in spanwise circulation (e.g. tip and root effect), are modeled intrinsically, where they are covered by engineering models or not covered at all in BEM.

For a free wake, the wake convection speed at each wake point is determined by the aggregate of the induced velocities from all vortices using the law of Biot and Savart. However, to reduce cpu-time it is also possible to prescribe the convection (Figure 2) for a specified number of wake points. The current prescription determines convection based on the induced velocity at the blade extrapolated using axial momentum theory. Alternatively it is possible to specify the near wake free and prescribe the far wake convection.

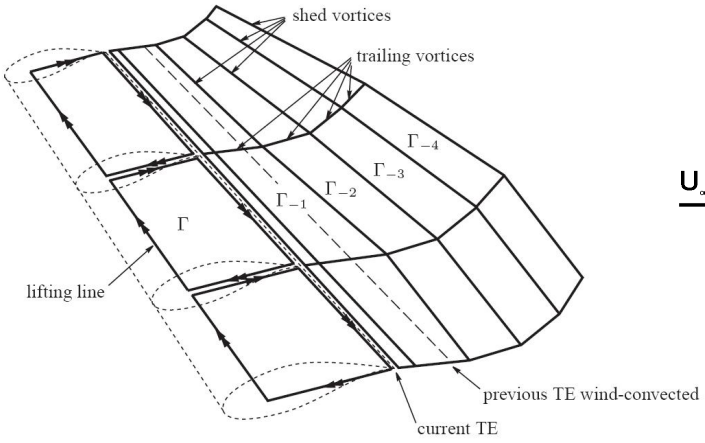

Figure 1. AWSM wake geometry [3]

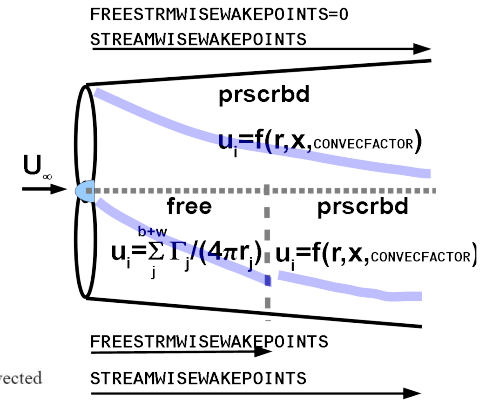

Figure 2. Wake modeling options (convective velocity in blue): Top half illustrates fully prescribed wake, lower half partially free/precribed wake

2.2. Simulation settings

Both the AVATAR [18] and INNWIND turbine [19] have been modeled for a variety of load cases. The turbines (including structural flexibility of blades, tower etc.) were modeled in accordance with the specified descriptions [18, 19]. For most of these cases three different aerodynamic solver settings have been applied, namely BEM, AWSM free wake and AWSM with a hybrid free and prescribed wake. For the free vortex wake simulation, the number of wake points was chosen to make sure that the wake length was developed over at least 3 rotor diameters downstream of the rotor plane. The wake convection was free for approximately 2 rotor diameters downstream. For the remaining diameter in the far wake, the blade average induction at the free to fixed wake transition is applied to all wake points. For the hybrid free and prescribed wake option the total wake length was kept the same but the number of free wake points was reduced to cover approximately one rotor revolution.

The Snel dynamic stall model [20] was applied to all simulations unless noted otherwise. Pitch angle and rotational speed were fixed for the sake of a sound comparison between the configurations. To ensure realistic conditions for the turbulent wind case a prescribed controller was adopted that forced rotational speed and pitch angle from a look-up table obtained from BEM simulations. For the pitch step case the rotational speed was constant and the time variation of the pitch angle was prescribed from the experiment.

3. Results

A selection of corresponding results is given below. Although both the AVATAR and INNWIND turbine have been simulated, results here are given for the INNWIND test cases as these give rise to the most interesting observations. Prior to the considered load cases, simulations were performed in axial inflow conditions with a constant wind. These revealed small to negligible differences in results between the three solver configurations, especially compared to the differences between them in the cases under investigation.

3.1. Yawed flow

Misaligning the turbine 30° to the flow creates large inflow variations during a rotor revolution. Here we can distinguish the advancing and retreating effect (upper and lower half of the rotor plane) and the skewed wake effect accounting for the variation of induction due to the skewed wake geometry. Where the first is accounted for intrinsically once wind vector and turbine geometry are properly modeled, the second effect needs an engineering method in BEM. The model as defined by Schepers [21, 22] and Glauert [23] are implemented here. These models modify the local induction as a function of annulus average induction, yaw angle, relative radius and azimuth angle. Where the Glauert model features a sinusodial variation of induction as induced by the tip vortex, the Schepers model is fitted by comparison to wind tunnel measured axial velocities, also modeling the effect of the root vortex. In the visualization of results, the Schepers model is the default option and the legends indicate when the Glauert model has been used. In addition to the unsteady variations also the average absolute level of the loads is not trivial in BEM as the underlying momentum equation is developed for axial flow and there is no uniform approach towards incorporating lateral momentum into the equations. Both of the above described shortcomings in BEM are however intrinsically modelled in AWSM.

Figure 3 shows the resulting image at 70%R for a case in partial load. Apart from the tower effect clearly visible at 180° azimuth for all simulations, large differences in induction variation exist, both between the two BEM simulations as well as between BEM and AWSM, and consequently loads. The difference between the two skewed wake models used for BEM can be explained by the different formulas and fitting constants used in the models both for amplitude and phase shifts as a function of azimuth angle. The partially prescribed wake option seems to perform well judging by the agreement with the free wake result. The effect on the

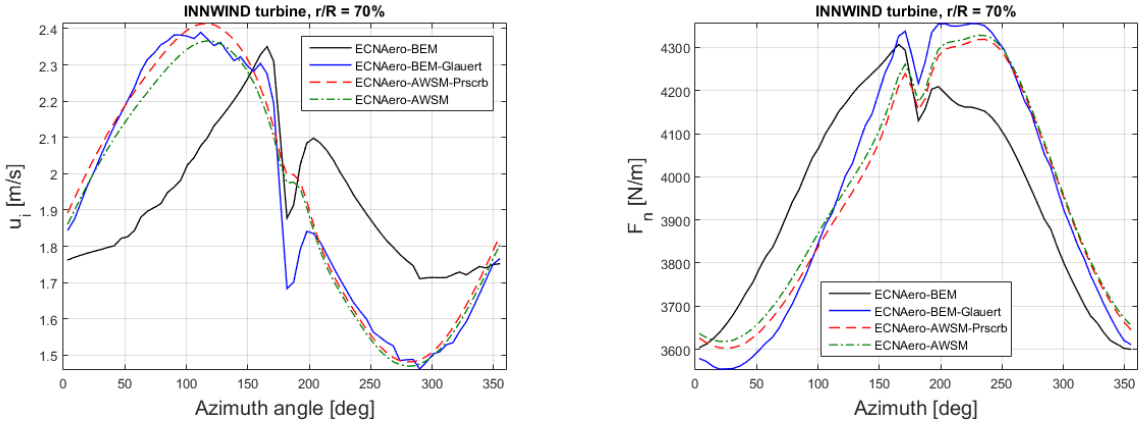

(a) Axial induction variation at 70%R

(b) Chord normal force at 70%R

Figure 3. Simulation results for 30° yaw, INNWIND rotor, U_∞=8m/s

damage equivalent flapwise moment was assessed. Referenced to the original BEM simulation, differences of -1%, -9% and -8% were found for the BEM Glauert, AWSM free wake and AWSM partially prescribed wake simulation respectively. This trend was observed to translate also into differences in the tower top and bottom moments. The power performance remained similar between the configurations.

3.2. Half wake

Several half wake simulations at various wake distances were performed, using deterministic wind profiles supplied by DTU [24]. A wind field visualization is given in Figure 4(a), showing large variations of inflow velocity over the rotor plane.

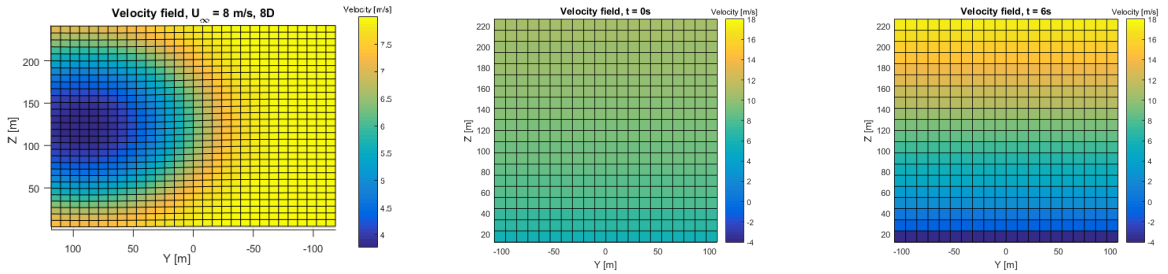

(a) Half wake at 8 diameters, U_∞=8 m/s

(b) Extreme wind shear, t=0 s, U_∞=9.4 m/s

(c) Extreme wind shear, t=6 s, U_∞=9.4 m/s

Figure 4. Visualization of wind field excitations, INNWIND rotor

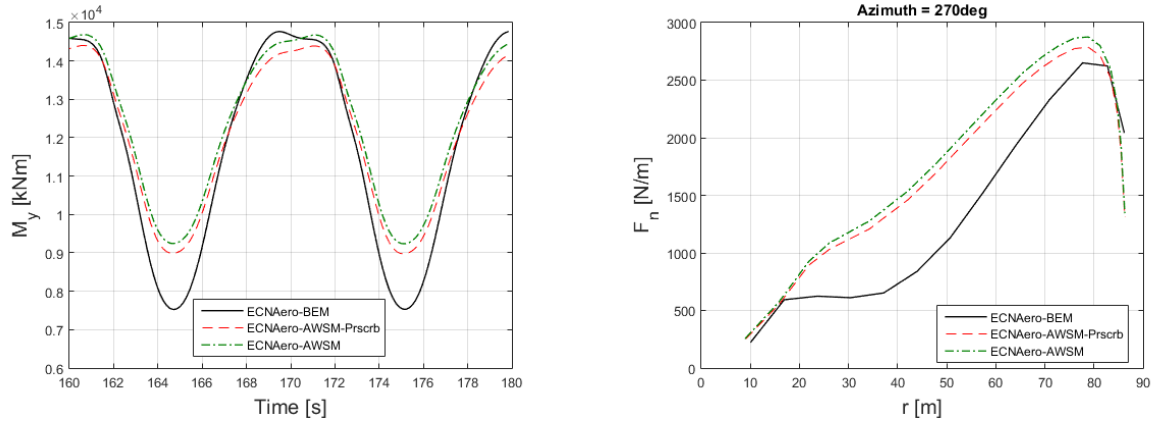

(a) Flapwise blade root moment as function of time

(b) Radial distribution of chord normal force at 270° azimuth

Figure 5. Simulation results for half wake at 8 diameters, INNWIND rotor, U_∞=8m/s

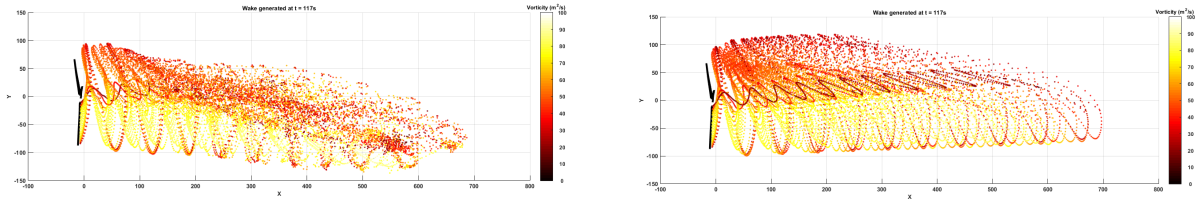

(a) Free wake

(b) Partially prescribed wake

Figure 6. Top view of wake geometry and vorticity, INNWIND rotor in half wake at 8 diameters, U_∞=8 m/s

For a particular case the results are shown in Figure 5. The dip in flapwise moment whilst sweeping through the wake is much more extreme for the BEM simulation. Zooming in on the normal force in the waked situation, not only the level but also the shape of the radial distribution is different for the BEM code. Non uniformity in the rotor plane is challenging for BEM type models, as interaction between the blades or annuli (radial) is not modeled. Here it must be noted that different implementations exist [25, 10], either calculating momentum equilibrium along a local streamtube or along a full annulus. The local approach was taken here, which is believed to be more physical especially in the case of non uniformity. But the implementation together

with a dynamic inflow model (which works on a whole annulus) is not straightforward and it is believed that steps can still be made here. Vortex models however are capable to implicitly model non uniformity effects both through lifting line (blades) and wake vortices induced velocities. The axial induced velocity follows the changes in the incoming wind better, resulting in a smaller angle of attack variation and consequently also load variation. The corresponding visualization of the wake geometry and vorticity is shown in Figure 6 for both the free as well as prescribed wake simulation. Although the near wake shows good agreement, the effect of prescription is clearly observed in the far wake preventing the wake to roll-up. The influence of this approximation on the loads remains small, because these are predominantly affected by the near wake vortices. Referenced to the original BEM simulation, staggering differences of -28% and -27% in the flapwise blade root fatigue equivalent moment were found for the AWSM free wake and AWSM partially prescribed wake simulation respectively. This trend was observed to translate also into differences in the tower top and bottom moments. Interestingly the average power production was found to increase around 5% for the free wake simulation, whilst accounting for differences in power production between the models that already existed in axial uniform inflow.

3.3. Extreme shear

Several extreme wind shear simulations were performed, using a deterministic wind. At t=0s an extreme shear transient is passing through the wind turbine rotor for several wind speeds and control parameters throughout the operational regime. Two snapshot illustration of the wind field around the passage of an extreme vertical shear are given in Figure 4(b) and 4(c). Hence instead of having a large horizontal wind gradient as for the half wake simulations, the non uniformity is now in the vertical direction. In addition to that there is a dynamic wake element added because of the transient nature of the extreme shear. Outside the passage of the transient a wind excitation featuring a normal vertical wind shear is acting on the turbine.

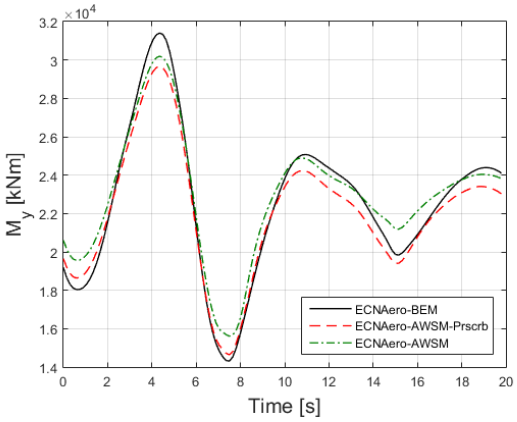

(a) Flapwise blade root moment as function of time

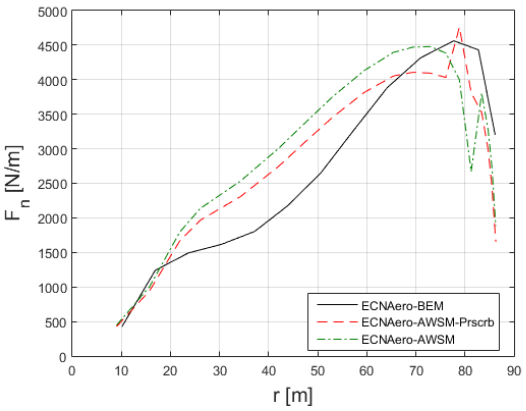

(b) Radial distribution of chord normal force at the drop in My (azimuth = 180°, t=7.5 s)

Figure 7. Simulation results for transient extreme vertical wind shear, INNWIND rotor, U_∞=9.4m/s

The simulation results for a particular case of the INNWIND rotor are illustrated in Figure 7. Similar to the half wake simulations, modeling the vortex wake reduces the amplitude of the load fluctuations caused by induced velocities better tracking the wind speed variation. The difference between the free or partially prescribed wake configuration is again small. A comparison of the normal force distribution at the drop in flapwise moment shows a similar

picture to the half wake case from Figure 5(b), with the exception of the sudden peaks near the tip probably caused by non-convergence. Referenced to the original BEM simulation, differences of -15% and -12% in the flapwise blade root fatigue equivalent moment were found for the AWSM free wake and AWSM partially prescribed wake simulation respectively (primarily induced by the normal shear acting outside of the transient). This trend was observed to translate also into differences in the tower top and bottom moments.

3.4. Turbulent inflow

A simulation featuring a stochastic wind excitation in accordance with IEC standards was performed for an average wind speed of 8 m/s and turbulence intensity of 23%. Both shear (exponent of 0.2) and uptilt (8°) were included in the wind field. Since the fast wind variations necessitate a smaller timestep than the other load cases, a compromise was made to obtain acceptable cpu-times. The time step was kept at 0.1 sec which roughly corresponds to 4° azimuth on average. In addition to that only 150 of the 600 seconds were simulated, leaving only the last 50 seconds for analysis due to the initialization taking the first 100 seconds. Settings were kept the same between the different solver configurations.

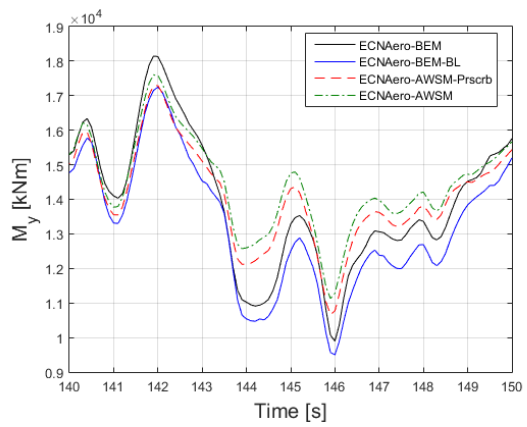

(a) Flapwise blade root moment as function of time

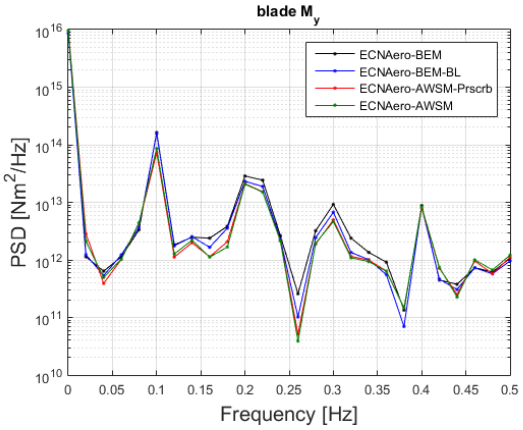

(b) PSD of flapwise blade root moment

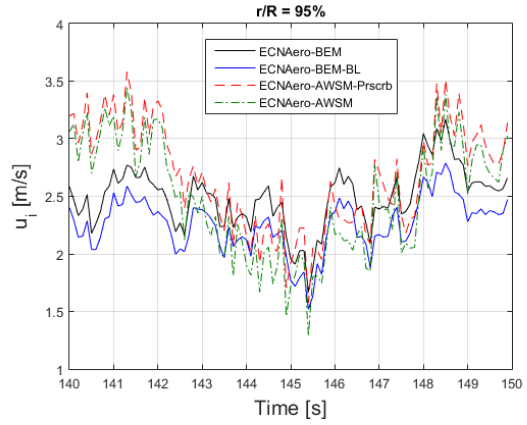

(c) Axial induced velocity at 95%R as function of time

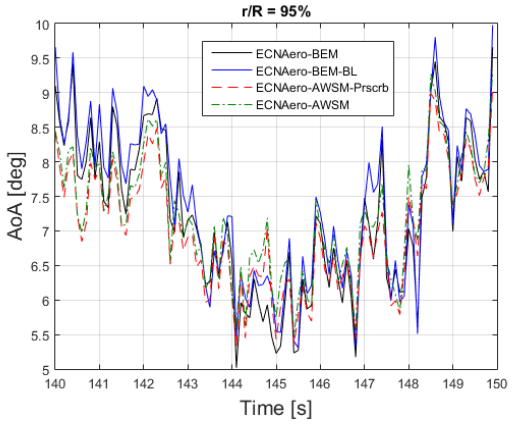

(d) Angle of attack at 95%R as function of time

Figure 8. Simulation results for turbulent inflow, INNWIND rotor, U_∞=8m/s

Figure 8 displays the results for the turbulent inflow case. The fluctuations in flapwise blade root moment are smaller yielding reduced peaks in the psd at the 1p, 2p and 3p frequencies

(the average rotor speed approximated 6 rpm). The variation in axial induction confirms that BEM is not able to adequately track inflow velocity changes as was noticed in the cases above, resulting in larger angle of attack changes. Since there is a continuous variation in shed vorticity for this case, the effect of using the Beddoes-Leishman [26, 27] instead of the Snel dynamic stall model was verified. This model contains a routine that corrects for shed vorticity effects in attached flow, which is implicitly included in the vortex wake method. Although the absolute level of the flapwise blade root moment time series in Figure 8(a) shows a larger offset to AWSM than the original BEM results (with Snel model applied), the fatigue loads (mainly related to load **variation**) come closer to the vortex wake result. Closer inspection of Figure 8(b) shows this difference to originate mainly from less unsteadiness in the 2p and 3p frequencies. However, judging by the unsteadiness in the 1p frequency, a large difference remains. The explanation lies in the momentum assumptions inherent to BEM based modeling, which balances the induced velocity field of an entire streamtube with the local blade forces. For a vortex wake model the effect of a different inflow velocity at the blade is treated much more local and hence induced velocities vary more directly with wind speed variations.

Referenced to the original BEM simulation, differences in blade flapwise fatigue equivalent load of -6%, -23% and -20% were found for the BEM Beddoes Leishmann, AWSM free wake and AWSM partially prescribed wake simulation respectively. This trend was observed to translate also into the tower top and bottom moments. The average power performance also varied between the configurations in agreement with the absolute level differences of flapwise moment of Figure 8(a). Considering the differences readily found in axial flow for deterministic wind, a decrease of 6% was found for the prescribed wake simulation and a decrease of 8% for the BEM simulation with the Beddoes Leishman model, whilst the power production for the free wake simulation remained similar compared to the original BEM simulation. Further investigation should clarify the cause for these rather large differences.

A question that can be raised when using vortex models in turbulent inflow conditions (but also e.g. in sheared inflow), relates to the fact that when modeling vorticity also vorticity in the inflow conditions should be taken into account. However the magnitude of this effect still awaits quantification. Furthermore it must be noted that due to the relatively small analysis time taken to deduce the fatigue loads (apart from the fact that only one wind seed was used), the numbers given for this load case must be interpreted with care. However the current aim is to identify differences between the used aerodynamic models rather than determine the absolute level of fatigue loads, which can partly justify this approach. Reducing the timestep from 0.10 s to 0.05 s was shown not to significantly influence the fatigue load results.

3.5. Pitch step

Finally a load cases was selected that allows comparison to experimental results. The New Mexico campaign [28] features rotor experiments in controlled conditions on a fully instrumented 4.5m diameter turbine featuring a 3 bladed rotor, see also Figure 9(a). The blades were equipped with unsteady pressure sensors to capture the temporal variation of aerodynamic loads. A dynamic pitch step was performed for several operating conditions, first pitching up from -2.3° to 5.0° and then pitching back again to 2.3°. The aim was to create a dynamic inflow effect challenging for dynamic load case modeling.

Result are shown in Figure 9 for an operational condition featuring a relative large axial induction factor ($\approx$0.4) in the turbulent wake state. The large level differences both between codes as well as codes to experiment can be explained by the difficulties both models have simulating the turbulent wake state together with a reduced experimental accuracy at this low freestream wind velocity. However, a clear dynamic inflow effect can be observed in the measured loads, slowly reaching an equilibrium state both for the pitch step up and down. The BEM results almost directly converge to a steady state, while it can be observed that the damping of the

vortex wake result is in better agreement with the experiment. This indicates that there is still room for improvement in the time constants used in the dynamic inflow engineering model. It is noted that the above results are in agreement with a comparison to the NREL UAE Phase VI experiment [9], which also featured a pitch step as reported in [6]).

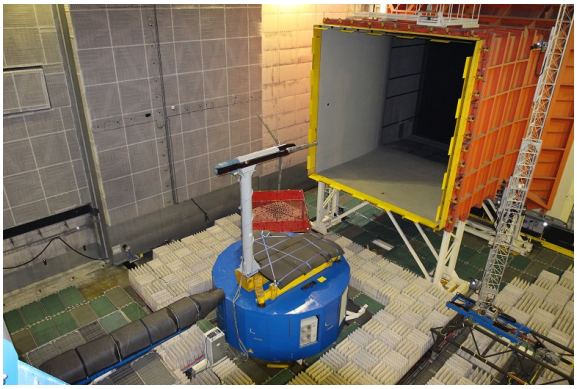

(a) Test set-up of New Mexico experiment

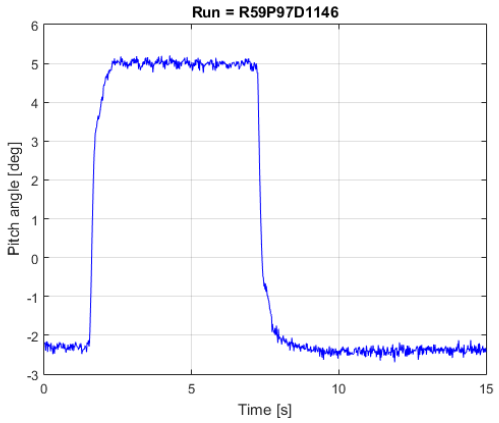

(b) Pitch angle excitation as a function of time

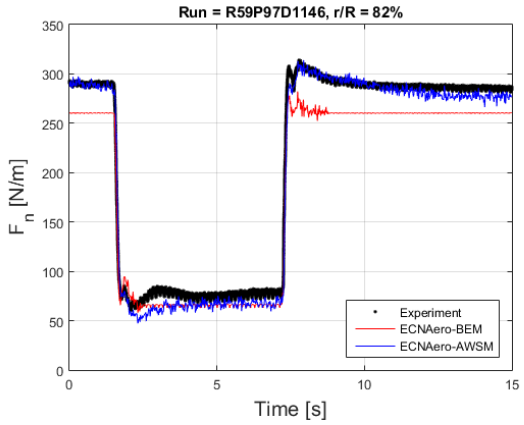

(c) Chord normal force at 82%R as a function of time

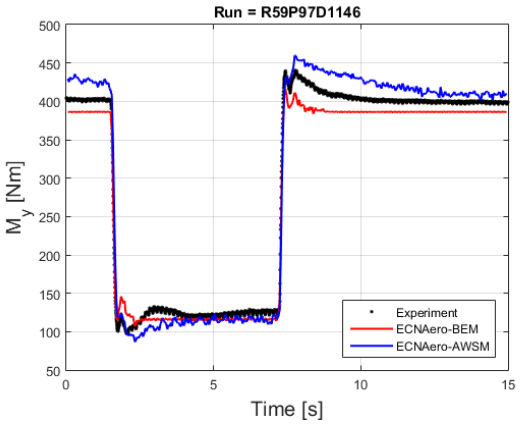

(d) Flapwise blade root moment (from pressures) as a function of time

Figure 9. Simulation results for the pitch step case, Mexico rotor, U_∞=10m/s, 424 rpm

3.6. Discussion

Differences between BEM and vortex wake modeling were exposed for a variety of dynamic load cases. Generally speaking significant variations were found in terms of fatigue loads. However, differences between BEM codes themselves are often of the same magnitude as was observed by a comparison with other partners within the AVATAR project. The advantage of the current comparison lies in the fact that external input and structural dynamics for both aerodynamic codes is exactly the same and observed differences can be stated to arise truly due to a different aerodynamic model. A comparison to measured values for the dynamic inflow case indicates that, although level differences exist, the dynamics as calculated by AWSM are more accurate than BEM. A validation by comparison to measurements can unfortunately not be performed for all load cases. It can be stated that the AWSM code is superior to BEM from a modeling point of view and the pitch step runs that have been performed in the wind tunnel during the

New Mexico campaign clearly point into this direction as well. As such it is believed that using higher fidelity models for selected load cases and wind turbines can improve design and loads verification featuring a lower uncertainty. In addition to that vortex models can aid to improve and calibrate the engineering models in BEM. Furthermore it is noted that differences between the models tend to increase for load case featuring high thrust coefficients (or axial induction factors). Consequently, the differences observed for the AVATAR rotor were smaller than the ones reported above for the INNWIND turbine.

The use of vortex models comes with a significant increase in CPU time, especially for dynamic load case simulation featuring a small time step. In addition to that many implicit calls to the aerodynamic routines are often required for a single timestep to reach equilibrium with the structural modeling. For a free vortex wake simulation, an average increase of a factor of 1500 was observed (accounting for approximately 30 hrs of CPU time for a 150 second simulation) compared to the BEM simulation. This figure includes the effect of parallelisation which reduced the CPU time by a factor of 4. The hybrid prescribed wake formulation was shown to further reduce this by a factor of 6, because the number of free wake points were decreased to cover only one rotor revolution. However this concept still uses a fine spatial and temporal resolution of vortices in the far wake. A promising concept to further reduce CPU time is represented by lumping far wake vorticity, for example using a cylindrical wake model.

4. Conclusions

In summary, the comparison to BEM indicates that vortex wake models can yield a significantly different aero-elastic response. As such it is believed that using higher fidelity models for selected load cases and wind turbines can improve design and loads verification featuring a lower uncertainty. Since dynamic inflow modeling for BEM has been developed for axi-symmetric wakes, it cannot account for non-uniform wakes and their effect on the rotor loading. For the considered cases, the more detailed wake geometry acts as a damper to fluctuations reducing fatigue loads, especially for rotors operating at high thrust coefficients. Modeling-wise the induced velocities track the wind speed variations better, resulting in smaller angle of attack variations and consequently smaller load fluctuations. However, differences between BEM codes themselves are often of the same magnitude as was observed by a comparison with other partners within the AVATAR project. The advantage of the current comparison lies in the fact that external input and structural dynamics for both aerodynamic codes is exactly the same and observed differences can be stated to arise truly due to a different aerodynamic model. Because a validation by comparison to measurements has not been performed for all load cases, it is difficult to prove that the AWSM results are more accurate than BEM. It can be stated that the AWSM code is superior to BEM from a modeling point of view and a comparison of the dynamic load variation from the pitch step runs that have been performed in the wind tunnel during the New Mexico campaign clearly point into this direction as well. Since the free vortex wake simulations come at a radical increase of cpu-time, a hybrid approach prescribing the far wake was shown to offer a promising compromise. Further improvements in this field could enable a more thorough verification of the performance of vortex wake models and evaluation of even more exotic load cases such as flutter calculations.

Acknowledgements

Financial support for this work was given in part by the EU AVATAR project.

References

[1] J.G. Schepers and K. Boorsma et al. Final report of IEA Task 29: Mexnext (Phase 2). ECN-E-14-060, Energy Research Center of the Netherlands, December 2014.

[2] J.G. Schepers and K. Boorsma et al. Final report of IEA Task 29, Mexnext (Phase 1): Analysis of MEXICO wind tunnel measurements. ECN-E-12-004, Energy Research Center of the Netherlands, February 2012.

[3] A. Van Garrel. Development of a wind turbine aerodynamics simulation module. Technical Report ECN-C–03-079, ECN, 2003.

[4] S. G. Voutsinas. Vortex methods in aeronautics: How to make things work. *International Journal of Computational Fluid Dynamics*, 20:3–18, 2006.

[5] S. Gupta. *Development of a Time-Accurate Viscous Lagrangian Vortex Wake Model for Wind Turbine Applications*. PhD thesis, University of Maryland, 2006.

[6] K. Boorsma, F. Grasso, and J.G. Holierhoek. Enhanced approach for simulation of rotor aerodynamic loads. Technical Report ECN-M–12-003, ECN, presented at EWEA Offshore 2011, Amsterdam, 29 November 2011 - 1 December 2011, 2011.

[7] S. Gupta and G.J. Leishman. Performance Predictions of the NREL Phase VI Combined Experiment Rotor Using a FreeVortex Wake Model. In *44th AIAA Aerospace Sciences Meeting and Exhibit*, January 2006.

[8] J.G. Schepers and H. Snel. MEXICO, Model experiments in controlled conditions. ECN-E-07-042, Energy Research Center of the Netherlands, 2007.

[9] M.M. Hand DA Simms, LJ Fingersh, DW Jager, JR Cotrell, S Schreck, and SM Larwood. Unsteady Aerodynamics Experiment Phase VI Wind Tunnel Test Configurations and Available Data Campaigns. NREL/TP-500-29955, National Renewable Energy Laboratory, NREL, December 2001.

[10] H.A. Madsen et al. BEM modeling of inflow with shear in comparison with advanced model results. In *Proceedings of The Science of Making Torque from the Wind*, June 2010.

[11] S. Hauptmann et al. Comparison of the lifting-line free vortex wake method and the blade-element momentum theory regarding the simulated loads of multi-mw wind turbines. *Journal of Physics: Conference Series*, 555, 2014.

[12] L. Oggiano, K Boorsma, J.G. Schepers, and M. Kloosterman. Comparison of simulations on the NewMexico rotor operating in pitch fault conditions. In *Proceedings of The Science of Making Torque from the Wind*, October 2016.

[13] H.D. Currin et al. Dynamic Prescribed Vortex Wake Model for AERODYN/FAST. *Journal of Solar Energy Engineering*, 120, August 2008.

[14] G. R. Pirrung, M. H. Hansen, and H. A. Madsen. Improvement of a near wake model for trailing vorticity. In *Proceedings of The Science of Making Torque from Wind*, 2012.

[15] C. Lindenburg and J.G. Schepers. Phatas-IV aeroelastic modelling, release "dec-1999" and "nov-2000". Technical Report ECN-CX–00-027, ECN, 2000.

[16] http://www.wmc.eu/focus6.php. 2016.

[17] H. Snel and J.G. Schepers. Joule1: Joint investigation of dynamic inflow effects and implementation of an engineering model. Technical Report ECN-C–94-107, ECN, 1994.

[18] `https://www.eera-avatar.eu/`, Password protected environment for exchange of AVATAR data. ECN.

[19] `http://dtu-10mw-rwt.vindenergi.dtu.dk/`, the DTU 10MW Reference Wind Turbine Project Site. DTU.

[20] H. Snel. Heuristic modelling of dynamic stall characteristics. In *Conference proceedings European Wind Energy Conference*, pages 429–433, Dublin, Ireland, October 1997.

[21] J.G. Schepers and Vermeer L.J. Een engineering model voor scheefstand op basis van windtunnelmetingen. Technical Report ECN-CX–98-070, ECN, 1998.

[22] J.G. Schepers. An engineering model for yawed conditions, developed on basis of wind tunnel measurements. Technical Report AIAA-1999-0039, AIAA, 1999.

[23] H. Glauert. A General Theory of the Autogyro. Technical Report ARC R&M No.1111, ARC R&M, 1926.

[24] T.J. Larsen. email with attachment 'deficits.zip'. email, DTU, August 2015.

[25] H.A. Madsen et al. *Influence of wind shear on rotor aerodynamics, power and loads*, pages 101–116. Risø National Laboratory, 2007. Risø-R-1611(EN).

[26] J.G. Leishman and T.K. Beddoes. A generalized method for unsteady airfol behaviour and dynamic stall using the indicial method. In *42nd Annual Forum*, Washington D.C., June 1986. American Helicopter Society.

[27] J.G. Leishman and T.K. Beddoes. A semi-empirical model for dynamic stall. *Journal of the American Helicopter Society*, 34:3–17, 1989.

[28] K. Boorsma and J.G. Schepers. New MEXICO Experiment, Preliminary overview with initial validation. Technical Report ECN-E–14-048, ECN, September 2014.